Journal of Catalysis **186,** 1–11 (1999)
Article ID jcat.1999.2531, available online at http://www.idealibrary.com on IDEAL®

# Effects of Pretreatment Conditions on CO Oxidation over Supported Au Catalysts

Eun Duck Park and Jae Sung Lee[1]

*Department of Chemical Engineering and School of Environmental Engineering, Pohang University of Science and Technology (POSTECH), San 31 Hyoja-Dong, Pohang 790-784, Republic of Korea*

Received May 11, 1998; revised March 25, 1999; accepted April 20, 1999

**Supported gold catalysts were prepared by a deposition–precipitation method and characterized to understand the different activities for CO oxidation with different pretreatment conditions. Gold catalysts supported on $Fe_2O_3$, $TiO_2$, and $Al_2O_3$ showed decreasing activity with increasing calcination temperatures, with the $Al_2O_3$-supported catalyst showing activity substantially lower than that of the other two catalysts. X-ray photoelectron spectroscopy (XPS) and X-ray absorption fine structure (XAFS) studies showed the phase transition of gold from $Au(OH)_3$ through $Au_2O_3$ to metallic gold with increasing calcination temperatures for all catalysts. In addition to the particle size of metallic gold, the oxidation states of gold were proven to be important for CO oxidation. The oxidized gold species were more active than metallic gold. Furthermore, facile formation of the interface between gold and support appears to be critical for high CO oxidation activity of supported gold catalysts.** 

*Key Words:* **CO oxidation; $Au/Fe_2O_3$; $Au/TiO_2$; $Au/Al_2O_3$; XAFS; XPS; oxidation state of gold.**

## INTRODUCTION

Gold has been regarded as a far less active catalyst than the platinum-group metals because of its chemically inert character and its low dispersion on common support materials (1). Therefore its use in catalysis has been restricted to a limited number of hydrogenation and oxidation reactions (1, 2). In general, these Au catalysts, commonly prepared by conventional impregnation techniques, are active only at elevated temperatures.

Recently, Haruta *et al.* (3–7) reported that gold particles smaller than 10 nm could be formed on $Co_3O_4$, $\alpha$-$Fe_2O_3$, NiO, and $Be(OH)_2$ through coprecipitation and that these Au catalysts were active in the oxidation of CO at a temperature as low as 200 K. For gold catalysts supported on $TiO_2$, $\alpha$-$Fe_2O_3$, and $Co_3O_4$, turnover rates for CO oxidation per surface gold atom were reported to be almost independent of the kind of support oxides used, yet they increased sharply with a decrease in the diameter of gold particles below 4 nm. Small gold particles not only provided sites for the reversible adsorption of CO but also appreciably increased the amount of oxygen adsorbed on the support oxides. These novel supported Au catalysts were reported to show increasing activity in the presence of water, unlike traditional metal oxide catalysts such as Hopcalite catalysts (mixed oxides composed mainly of Mn and Cu), but in agreement with more recently reported catalysts for low-temperature CO oxidation such as Pt or $Pd/SnO_2$ (8) and supported $PdCl_2$–$CuCl_2$ catalysts (9–11). Haruta and co-workers (12, 13) studied the relation between the particle size of Au and the calcination conditions for $TiO_2$-supported Au catalysts prepared by deposition–precipitation. They also observed that physically mixed Au and $TiO_2$ samples showed a low catalytic activity, yet exhibited gradual improvement with increasing calcination temperatures. It was concluded that the catalytic activity of $Au/TiO_2$ was sensitive to the structure of the perimeter interface between Au and $TiO_2$. Bollinger *et al.* (14, 15) reported that even impregnated $Au/TiO_2$ could become active catalysts after sequential pretreatments consisting of high-temperature reduction at 773 K, calcination at 673 K, and low-temperature reduction at 473 K but that deactivation was observed over a long period of time under reaction conditions. They also found that deposition of $TiO_x$ overlayers onto an inactive Au powder produced high activity (15). From these findings they argued that an electronic effect of small Au particles was not the major factor contributing to the unusual activity of $Au/TiO_2$ catalysts but more important was the formation of active sites at the $Au/TiO_2$ interface produced by the mobility of $TiO_2$ species.

Pantelouris *et al.* (16) conducted the X-ray absorption spectroscopy for various Au compounds and reported that the absorption edge shift was not directly observable in the Au $L_{III}$ X-ray absorption near edge structure (XANES) spectra for the $Au^0$, $Au^+$, and $Au^{3+}$ compounds. In X-ray absorption fine structure (XAFS) studies of impregnated $Au/\gamma$-$Al_2O_3$ and Au/MgO catalysts (17, 18), two distinct phases of gold were found. A part of gold was structurally

[1] To whom all correspondence should be addressed.



0021-9517/99 $30.00

similar to metallic Au; the rest was present in the form of either two-dimensional or atomically dispersed clusters, carrying a formal charge of +1. A study of Au $L_{III}$ XAFS was made on ultrafine gold particles supported on beryllium hydroxide ($Au/Be(OH)_2$) and magnesium hydroxide ($Au/Mg(OH)_2$) (19). It was proposed that the catalytic activity for CO oxidation arose from the presence of Au–Au coordination in $Au/Be(OH)_2$ and $Au/Mg(OH)_2$, although in the latter Au–Au and Au–O coordination coexisted in the most active catalysts. Surface characterization of supported Au catalysts with X-ray photoelectron spectroscopy (XPS) has been conducted. Gardner *et al.* (20) examined $Au/MnO_x$ before and after pretreatment in He at 328 K and reported that the pretreatment enriched the gold part of the surface of this catalyst and decreased the surface oxygen concentration on $MnO_x$. Epling *et al.* (21) reported that the near-surface region of the $Au/\alpha$-$Fe_2O_3$ catalyst contained more Au than that of the $Au/Co_3O_4$ catalyst and that Au was present as gold crystallites with small amounts of $Au(OH)_3$. Haruta *et al.* (7) observed gold clusters lying electronically between metal $Au^0$ and cations $Au^+$ or $Au^{3+}$ in Au–Fe coprecipitates that were calcined at 573 K. However, these materials were not catalytically more active than the samples without gold clusters. From this result, they concluded that metallic Au particles were responsible for CO oxidation.

Until now, the active phase of gold has been studied with catalysts prepared mostly by coprecipitation whose surface area and exposed gold concentration changed with pretreatment conditions. Even for $TiO_2$-supported Au catalysts prepared by deposition–precipitation, the catalytic activity has been compared after fully reducing gold compound into metallic Au (12, 13). This might have made the conclusions regarding the active phase of gold equivocal. In this study, similar surface areas and exposed gold concentrations are established by preparing catalysts with the deposition–precipitation method where gold particles deposit onto a preformed oxide from a Au-containing solution. In addition to known active supports of $TiO_2$ and $Fe_2O_3$, gold supported on $\gamma$-$Al_2O_3$ is also studied for comparison. The effects of the oxidation state of gold on the catalytic activity for CO oxidation in dry and wet conditions are studied.

## EXPERIMENTAL

### *Preparation of Catalysts*

The deposition–precipitation method was used to prepare the supported Au catalysts. Support materials were $Al_2O_3$ (Alfa, surface area = 170 $m^2/g$), $TiO_2$ (JRC-$TIO_4$, surface area = 50 $m^2/g$), and $Fe_2O_3$ (calcined at 873 K after precipitation from $Fe(NO_3)_2 \cdot 6H_2O$ with 1 N NaOH, surface area = 16 $m^2/g$). Gold precursor was $HAuCl_4 \cdot 3H_2O$ (Aldrich, 99.9%). Each of these supports was dispersed in an aqueous solution of $HAuCl_4$ at 343 K. The pH of the support dispersion was adjusted to 8 with the addition of 0.1 N NaOH. This aqueous dispersion was stirred for 2 h at the adjusted pH, filtered, and then washed with hot distilled water several times to remove residual $Cl^-$ species. The cake was dried at 373 K in a dry oven and calcined for 5 h at different temperatures and under different conditions.

The gold contents were determined with Perkin–Elmer AAS 5100PC. $TiO_2$- and $Fe_2O_3$-supported Au catalysts containing Au contents high enough for spectroscopic characterizations showed such high activities that it was impossible to carry out rate measurements over the desired temperature range. Therefore, two kinds of catalysts were prepared with different gold contents for each support. The catalyst with the lower Au loading was prepared for the activity test in dry and wet conditions and the catalyst with the higher Au loading was prepared for spectroscopic characterizations. Gold loadings were 0.15 and 0.21 wt% for $TiO_2$-supported Au catalysts and 0.26 and 1.16 wt% for $Fe_2O_3$-supported Au catalysts. The 1.85 wt% gold loading was used for $Al_2O_3$-supported catalysts for both purposes.

### *CO Oxidation*

The rates of CO oxidation were measured in a small fixed-bed reactor packed with catalyst powders of 100/120 mesh. A standard feed gas of 1.0 vol% CO and 10 vol% (or 5 vol%) $O_2$ balanced with nitrogen was passed through the catalyst bed at atmospheric pressure. All the experiments in the dry condition were performed after pretreatment of the sample with air at 373 K for 1 h to remove adsorbed $H_2O$. For activity tests under the wet condition, the reaction gases were directed through a water vapor saturator immersed in a constant temperature bath and fed to a reactor through a glass line warmed by a heating tape. The conversion of CO was determined through gas chromatographic analysis (HP5890A, molecular sieve 13X column) of the effluent from the reactor. The reaction rates were measured under the conditions of an integral condition in the presence of an excess of oxygen. It has been reported that the reaction rate is slightly dependent on the concentration of $O_2$ over this type of catalyst (7).

### *Characterization of Catalysts*

X-ray photoelectron spectroscopy (XPS) measurements were conducted with a Perkin–Elmer PHI 5400 ESCA spectrophotometer with monochromatic Mg $K\alpha$ radiation (1253.6 eV). After fresh catalysts were treated under different gas flows and at different temperatures, they were pressed into a pellet and transferred to a test chamber. Spectra were collected with an analyzer pass energy of 89.45 eV and an electron takeoff angle of 70°. The vacuum in the test chamber during the collection of spectra

was maintained below $5 \times 10^{-9}$ Torr. Sun Sparc Station 4 was utilized for data acquisition and curve fitting. Binding energies were corrected for surface charging by referencing them to the energy of C1*s* peak of contaminant carbon at 285.0 eV. The XPS Au 4*f* binding energies of bulk metallic Au, $Au_2O_3$, and $Au(OH)_3$ are 83.9, 86.3, and 87.7 eV for $4f_{7/2}$ and 87.7, 89.6, and 91.4 eV for $4f_{5/2}$, respectively. The $4f_{5/2}$ and $4f_{7/2}$ doublet corresponds to final states with total angular momentum $J_- = L - S = 5/2$ and $J_+ = L + S = 7/2$, respectively. The intensity ratio of these lines is given by the ratio $(2J_- + 1)/(2J_+ + 1)$. Thus, the value is 3 : 4 for $f_{5/2}$ to $f_{7/2}$. We made an attempt to decompose the two envelopes of multiplet peaks by fixing components at 83.9, 86.3, 87.7, 89.6, and 91.4 eV using a curve fitting procedure based on a nonlinear least-square algorithm (22). Because the component at 87.7 eV reflects both metallic Au and $Au(OH)_3$, the intensity ratio described above was taken into account when this peak was deconvoluted. The homogeneous assumption was adopted for sensitivity factors of Au compounds.

The XAFS spectra were taken in a transmission mode for the $L_{III}$-edge of Au at beamline 10B of the Photon Factory in the National Laboratory for High Energy Physics (KEK) operating at 2.5 GeV with ca. 250–350 mA of stored current. The detector gases were Ar (15%) + $N_2$ (85%) for the incident beam and Ar (50%) + $N_2$ (50%) for the transmitted beam. The samples were pressed into thin self-supporting wafers and mounted in a Pyrex controlled atmosphere spectroscopic cell with Kapton windows where the sample could be treated under different gas flows and temperatures. Spectra of the Au $L_{III}$ edge were recorded at room temperature after pretreatment in air and during CO oxidation reaction for the samples still under the atmosphere of treating gases in the cell. In addition to catalysts samples, XAFS data were also obtained for Au foil, $Au_2O_3$, and $Au(OH)_3$ samples as references. They were analyzed by the UWXAFS 3.0 package licensed from University of Washington. The standard analysis procedure is described elsewhere in detail (23).

Bright-field images of transmission electron microscopy (TEM) were obtained using a Philips CM 200 TEM operated at 200 kV. Samples were finely ground in a mortar to fine particles and then dispersed ultrasonically in methanol. The sample was deposited on a Cu grid covered by a holely carbon film for measurements. The mean diameter of the Au particles was determined by observation of more than 100 particles.

## RESULTS

### *Au/$TiO_2$ Catalysts*

The rates of CO oxidation over Au/$TiO_2$ shown in Fig. 1 indicate that with increasing calcination temperatures the catalytic activity decreases in both the presence (the wet condition) and the absence (the dry condition) of water vapor. In all cases, the wet condition gave higher reaction rates. Figure 2 shows that the rates of CO oxidation are lower upon pretreatment in the reducing condition than in the inert condition, and the oxidizing pretreatment of the catalyst gave the highest activity. Each curve in Figs. 1 and 2 was acquired successively without intermittent air exposure between dry and wet conditions for the same catalyst. The reaction rates in the wet condition were the same as those

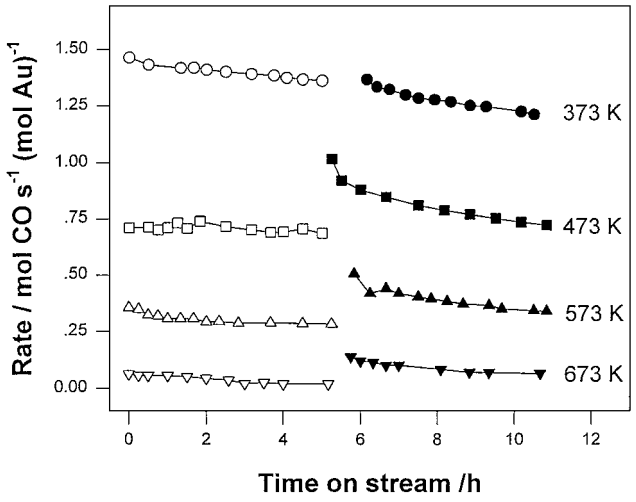


**FIG. 1.** The rate of CO oxidation at 323 K over Au/$TiO_2$ catalyst containing 0.15 wt% Au prepared at different calcination temperatures. The reactants, 1 vol% CO and 5 vol% $O_2$ in $N_2$, were fed directly to the catalyst in the dry condition (open points) and the reactants were directed through a water vapor saturator maintained at 273 K to obtain the wet condition (filled points).

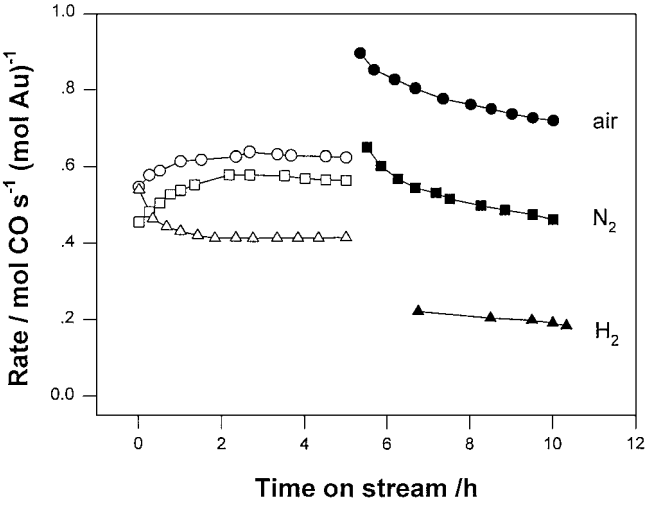


**FIG. 2.** The rate of CO oxidation at 303 K over Au/$TiO_2$ catalyst containing 0.15 wt% Au prepared at different calcination atmospheres at a fixed calcination temperature of 373 K. The reactants, 1 vol% CO and 5 vol% $O_2$ in $N_2$, were fed to the catalyst in the dry condition (open points) and the reactants were directed through a water vapor saturator maintained at 273 K to obtain the wet condition (filled points).

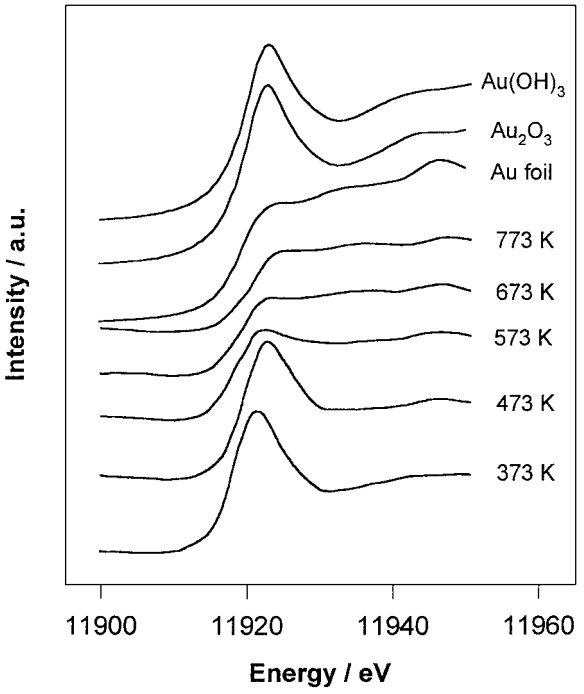


**FIG. 3.** Au $L_{III}$ XANES of $Au/TiO_2$ catalysts containing 0.21 wt% Au prepared with increasing calcination temperatures and Au reference samples.

obtained when the previous 5 h of dry reactions were omitted. To obtain information on the state of gold in $Au/TiO_2$ catalysts, the technique of X-ray absorption near edge structure (XANES) was employed. Figure 3 compares Au $L_{III}$ XANES of this catalyst prepared at increasing calcination temperatures with those of some reference compounds, Au foil, $Au_2O_3$, and $Au(OH)_3$. The gold phase was changed from an oxidized gold phase to metallic Au as the calcination temperature increased. The presence of the metallic Au phase was evident after calcination at 573 K or above.

*$Au/Fe_2O_3$ Catalysts*

The rates of CO oxidation over $Au/Fe_2O_3$ shown in Fig. 4 indicated that with increasing calcination temperatures the catalytic activity decreased in both the presence and the absence of water vapor. Again, the wet condition gave higher rates of CO oxidation. For this catalyst, any meaningful XANES spectra could not be obtained because of the low gold content and an excessive X-ray absorption by $Fe_2O_3$. Therefore, the technique of XPS was employed to obtain information on the state of gold in $Au/Fe_2O_3$ catalysts. Figure 5 compares XPS of Au 4*f* for these catalysts prepared at increasing calcination temperatures. The $Au/Fe_2O_3$ catalyst calcined at 373 K shows the peaks at 86.5 and 90.1 eV for Au $4f_{7/2}$ and Au $4f_{5/2}$ lines, respectively. These binding energies are close to Au 4*f* binding energies of $Au_2O_3$. After pretreatment with air at 473 K, three broad peaks appeared near Au 4*f* binding energies of $Au_2O_3$ and metallic Au. This can be interpreted as $Au_2O_3$ and metallic Au coexisting. For $Au/Fe_2O_3$ catalysts calcined above 573 K, two distinct peaks appeared at 84.3 and 87.9 eV, which were close to Au 4*f* binding energies of metallic Au. Therefore the gold phase was found to be changed from $Au_2O_3$ to metallic Au as the calcination temperature for $Au/Fe_2O_3$ catalysts increased. Pure metallic Au phase was formed upon calcination above 573 K. XPS spectra were also obtained to determine the oxidation states of Au after CO oxidation at 363 K for $Au/Fe_2O_3$ catalysts that had been calcined at 373 K. As shown in Fig. 5, the results depended on whether the reaction took place in the dry or the wet condition. In the dry condition, two distinct peaks appeared at 84.1 and 87.8 eV, which were close to Au 4*f* binding energies of metallic Au. Thus, the oxidized gold phase was reduced almost completely to metallic Au during the reaction. However, about 40% of the gold remained as $Au_2O_3$ after the reaction in the wet condition. Hence, an important role of water appears to suppress the reduction of gold during the reaction. To determine the relative portion

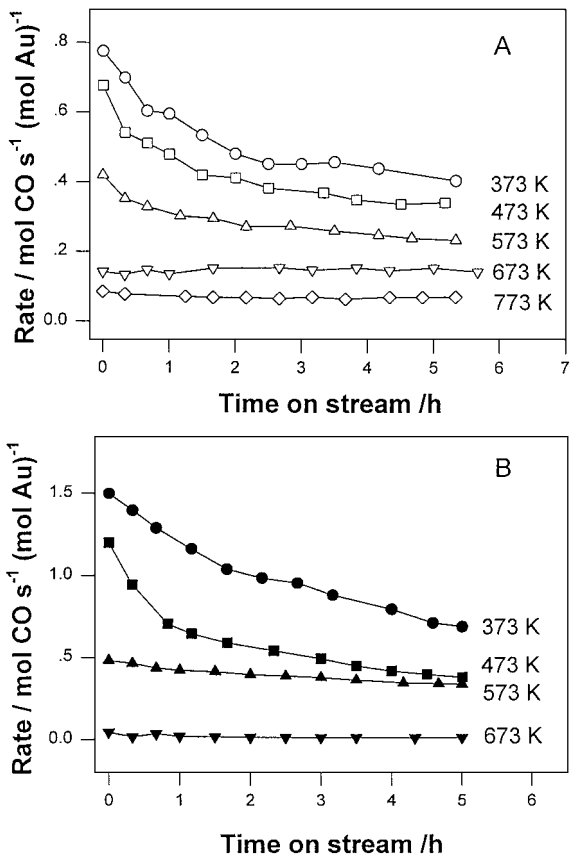


**FIG. 4.** The rate of CO oxidation at 363 K over $Au/Fe_2O_3$ catalyst containing 0.26 wt% Au prepared at different calcination temperatures. The reactants, 1 vol% CO and 10 vol% $O_2$ in $N_2$, were fed to the catalyst in the dry condition (A) and the reactants were directed through a water vapor saturator maintained at 278 K to obtain the wet condition (B).

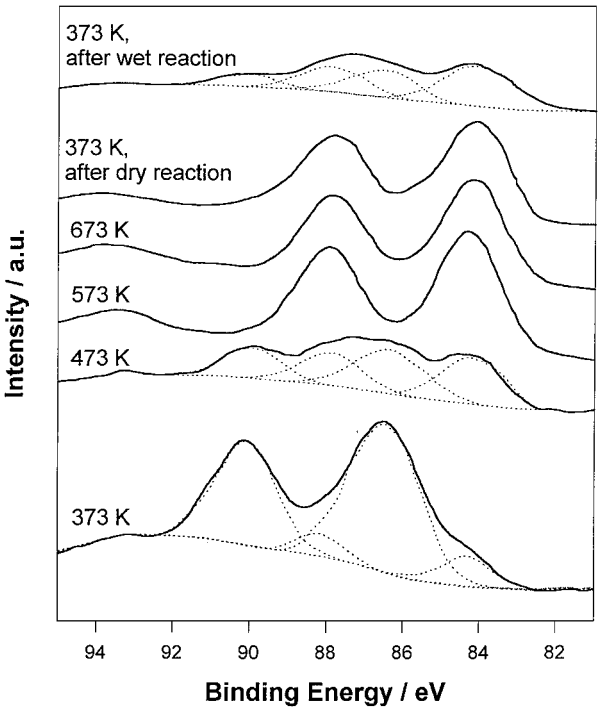


**FIG. 5.** XPS of Au 4*f* obtained for 1.16 wt% $Au/Fe_2O_3$ catalysts prepared at increasing calcination temperatures. The catalyst calcined at 373 K was used for CO oxidation at 313 K for 10 h in dry and wet conditions.

of $Au_2O_3$ and metallic Au quantitatively, deconvolution of Au 4*f* peaks was conducted, and the results are listed in Table 1. It also showed that the gold phase was transformed progressively from $Au_2O_3$ to metallic Au as the calcination temperature increased. Pure metallic Au phase was formed after calcination above 573 K.

Figure 6 shows bright-field images of $Au/Fe_2O_3$ catalysts prepared at increasing calcination temperatures in air. At the calcination temperature 373 K, the particle size of Au was too small to be observed. However, it appeared to increase with increasing calcination temperatures and Au particles were seen for catalysts calcined above 573 K. The mean diameters of Au particles in catalysts calcined at 573 and 773 K were estimated by averaging diameters of more than 100 individual particles and they were about 4 and 6 nm, respectively.

**TABLE 1**

**Surface Composition of $Au/Fe_2O_3$ Catalysts Prepared with Different Calcination Temperatures Obtained by Deconvolution of Au 4*f* Peaks**

| Calcination temperature (K) | $Au_2O_3$ | Au metal |
|---|---|---|
| 373 | 0.86 | 0.14 |
| 473 | 0.59 | 0.41 |
| 573 | 0.0 | 1.0 |
| 673 | 0.0 | 1.0 |

*$Au/Al_2O_3$ Catalysts*

The rate of CO oxidation over $Au/Al_2O_3$ in the dry condition exhibited the same trend as $TiO_2$- and $Fe_2O_3$-supported gold catalysts with calcination temperatures when

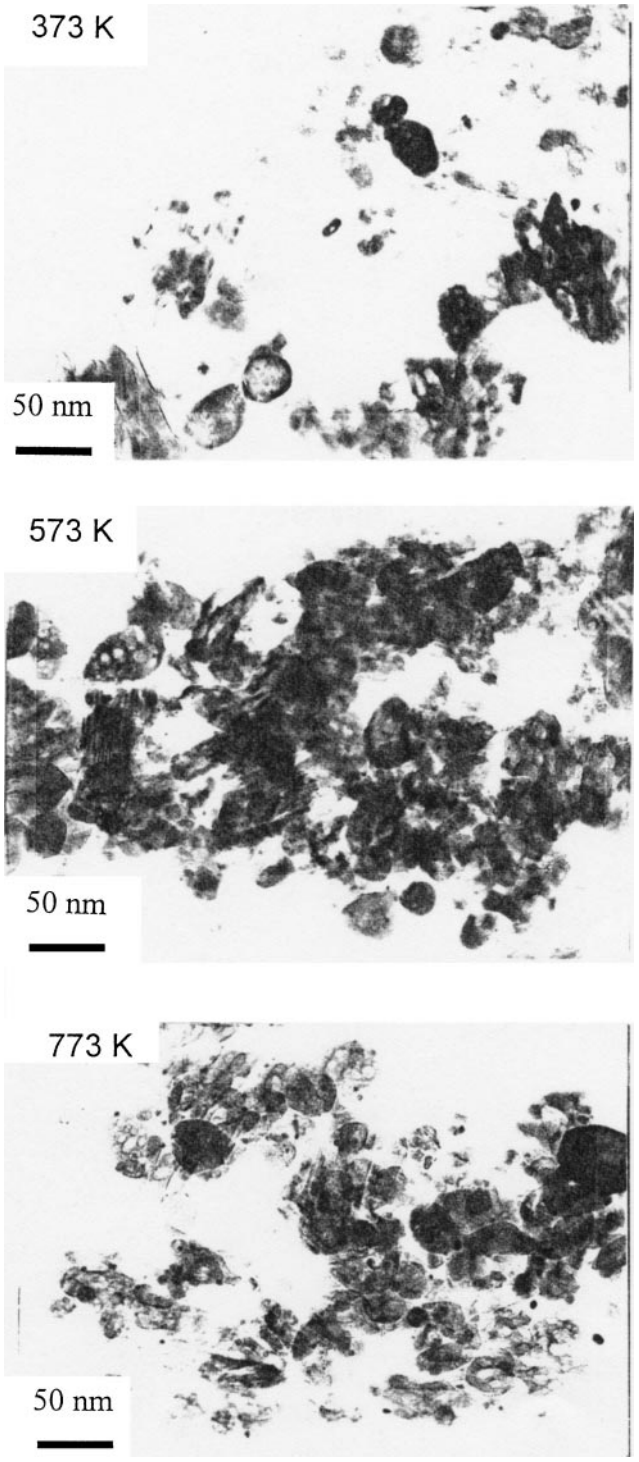


**FIG. 6.** TEM images of $Au/Fe_2O_3$ prepared at increasing calcination temperatures.

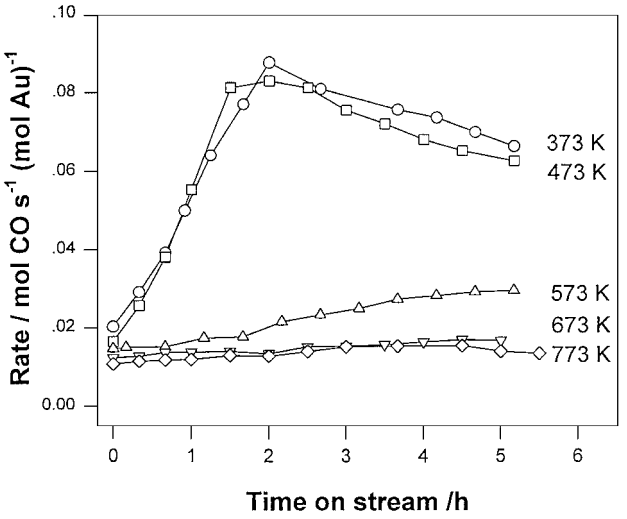


**FIG. 7.** The rate of CO oxidation at 318 K in the dry condition over $Au/Al_2O_3$ catalyst containing 1.85 wt% Au prepared at different calcination temperatures. Reactants: 1 vol% CO and 10 vol% $O_2$ in $N_2$.

pretreatment temperatures were higher than 573 K as shown in Fig. 7. For catalysts calcined below 473 K, however, the catalytic activity increased with time on stream and reached maximum values and decreased to the steady-state activities in dry conditions. In general, $Au/Al_2O_3$ catalysts showed catalytic activity at least an order of magnitude lower than that of $Au/TiO_2$ and $Au/Fe_2O_3$. To obtain information on the state and structure of gold in $Au/Al_2O_3$ catalysts, the technique of XAFS was employed. Figure 8 compares Au $L_{III}$ XANES of these catalysts prepared at different calcination temperatures with those of some reference compounds, Au foil, $Au_2O_3$, and $Au(OH)_3$. The results indicated that the gold phase was changed from $Au(OH)_3$ or $Au_2O_3$ to metallic Au. Again the presence of the metallic gold phase was evident after calcination above 673 K.

Small oscillations above the absorption edge were isolated from the background absorption. This extended X-ray absorption fine structure (EXAFS) was weighted with $k^3$ ($k$/Å$^{-1}$ = wave factor) and Fourier-transformed to obtain a radial structure function (RSF). Major peaks in the RSF correspond to important interatomic distances shifted from their true positions by phase shifts. The RSFs of reference compounds Au foil, $Au_2O_3$, and $Au(OH)_3$ are shown in Fig. 9. The main peaks correspond to distances of Au–Au (0.270 nm) and Au–O (0.160 nm). Phase shifts for those atomic pairs could be calculated from the differences between these distances and the known true distances for these compounds. The RSFs of $Au/Al_2O_3$ prepared at increasing calcination temperatures are shown in Fig. 10. In $Au/Al_2O_3$ calcined below 473 K, the major peak was observed at 0.157 nm. In comparison with the RSFs of the reference compounds in Fig. 9, gold is believed to be present as $Au_2O_3$ or $Au(OH)_3$ in these samples. However, as the

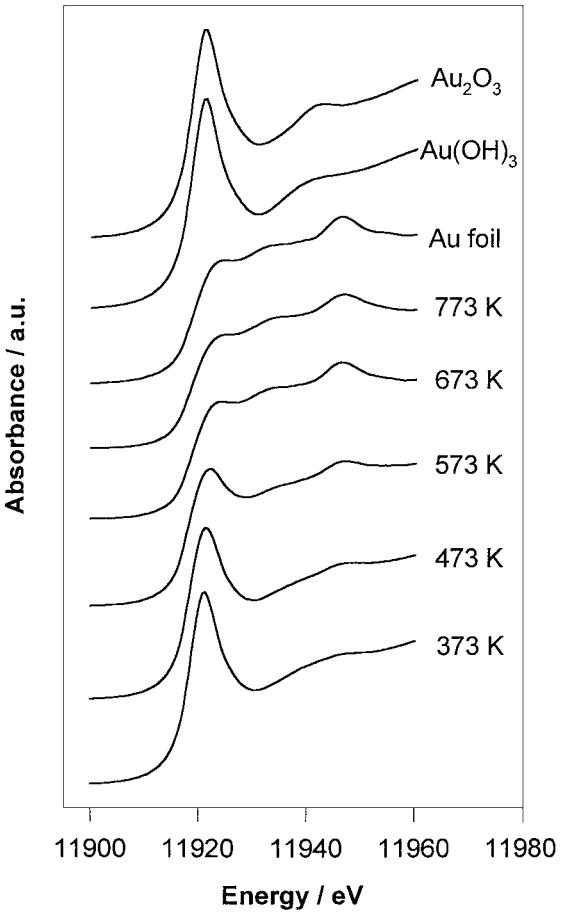


**FIG. 8.** Au $L_{III}$ XANES of $Au/Al_2O_3$ catalysts prepared at increasing calcination temperatures and Au reference samples.

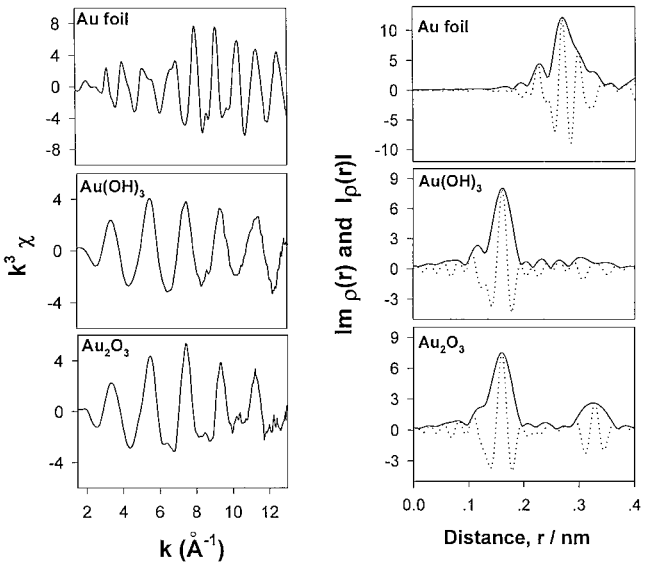


**FIG. 9.** $k^3$-weighted EXAFS functions and their Fourier transformation about the Au $L_{III}$-edge of Au reference samples. The imaginary part of Fourier transform is plotted with dashed lines.

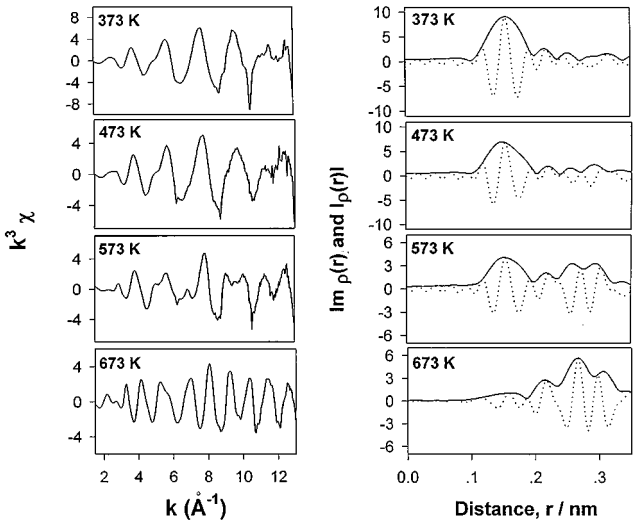


**FIG. 10.** $k^3$-weighted EXAFS functions and their Fourier transformation about the Au $L_{III}$-edge of $Au/Al_2O_3$ prepared at increasing calcination temperatures. The imaginary part of Fourier transform is plotted with dashed lines.

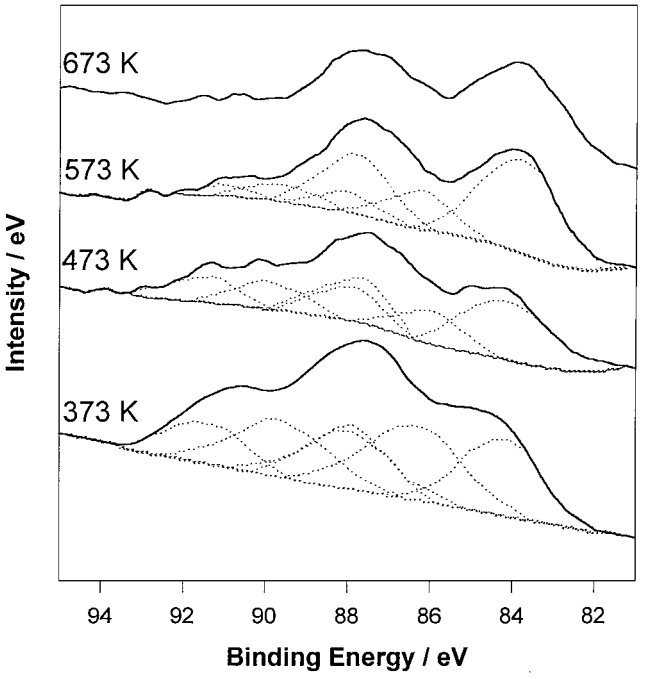


**FIG. 11.** XPS of Au 4*f* obtained for $Au/Al_2O_3$ catalysts prepared at increasing calcination temperatures.

calcination temperature increased above 573 K, intensities of peaks representing oxidized gold decreased and new peaks appeared around 0.270 nm, which could be assigned to Au–Au distances in gold metal. This indicated that the Au phase was changed from $Au(OH)_3$ or $Au_2O_3$ to metallic Au as the calcination temperature increased. In agreement with XANES results, the presence of metallic Au was observed after calcination above 673 K.

To obtain information on the surface state of gold in $Au/Al_2O_3$ catalysts, XPS study was carried out. Figure 11 compares XPS spectra of Au 4*f* for these catalysts prepared at increasing calcination temperatures. For $Au/Al_2O_3$ catalysts calcined below 573 K, three broad peaks appeared over the Au 4*f* region which could be deconvoluted to components due to $Au(OH)_3$, $Au_2O_3$, and metallic Au. These three components coexisted in these catalysts. For the $Au/Al_2O_3$ catalyst calcined at 673 K, two distinct peaks appeared at 84.0 and 87.8 eV, which were close to the Au 4*f* binding energies of metallic Au. Therefore the gold phase was found to be changed from $Au(OH)_3$ through $Au_2O_3$ to metallic Au as the calcination temperature for $Au/Al_2O_3$ catalysts increased. The relative fractions of $Au(OH)_3$, $Au_2O_3$, and metallic Au obtained by deconvolution of Au 4*f* peaks are listed in Table 2. It also shows quantitatively that the gold phase is transformed from $Au(OH)_3$ into $Au_2O_3$ and then to metallic Au as the calcination temperature increases. A difference from the result obtained for $Au/Fe_2O_3$ was that a significant fraction of metallic gold was present already in the $Au/Al_2O_3$ catalyst calcined at 373 K. The complete conversion to metallic gold took place upon calcination at 673 K.

The $Au/Al_2O_3$ catalyst showed an unusual temperature dependence in the wet condition as shown in Fig. 12. The catalyst initially showed a complicated activity pattern with calcination temperatures showing the highest rate of CO oxidation at 283 K for the catalyst calcined at 573 K, although the difference in rates was small. After the reaction at 283 K, the reaction temperature of CO oxidation increased to 328 K. After 2 h of the reaction at 328 K, the reaction temperature was brought down to 283 K again. After the intervening high-temperature reaction, the activity of the catalysts calcined below 573 K containing $Au_2O_3$ and $Au(OH)_3$ increased dramatically. Now the activity of $Au/Al_2O_3$ became comparable to that of $Au/TiO_2$ and $Au/Fe_2O_3$. However, the catalysts calcined at 673 K in which gold was present in metallic state showed no difference in activity before and after the high-temperature reaction. Hence, the activity pattern with calcination temperature for $Au/Al_2O_3$ became the same as the patterns for

**TABLE 2**

**Surface Composition of $Au/Al_2O_3$ Catalysts Prepared with Different Calcination Temperatures Obtained by Deconvolution of Au 4*f* Peaks**

| Calcination temperature (K) | $Au(OH)_3$ | $Au_2O_3$ | Au metal |
|---|---|---|---|
| 373 | 0.23 | 0.43 | 0.34 |
| 473 | 0.32 | 0.19 | 0.49 |
| 573 | 0.06 | 0.25 | 0.69 |
| 673 | 0.0 | 0.0 | 1.0 |

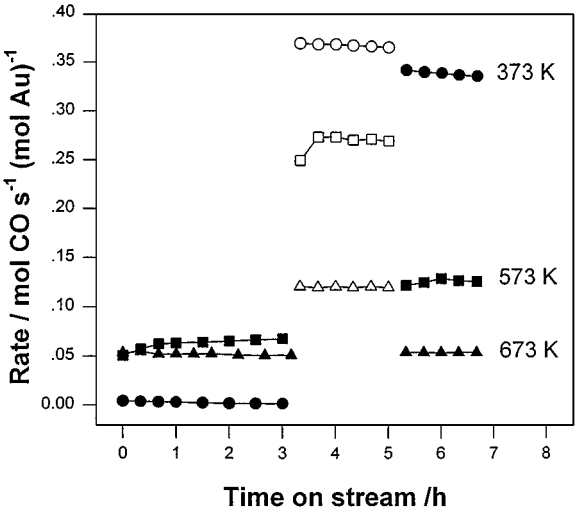


**FIG. 12.** The rate of CO oxidation in the wet condition at different tempratures of 283 K (filled points) and 328 K (open points) over $Au/Al_2O_3$ catalyst containing 1.85 wt% Au prepared at different calcination temperatures. The reactants, 1 vol% CO and 10 vol% $O_2$ in $N_2$, were fed to the catalyst through a water vapor saturator maintained at 278 K.

$Au/TiO_2$ and $Au/Fe_2O_3$, i.e., a lower activity for catalyst calcined at a higher temperature. The RSFs of $Au/Al_2O_3$ calcined at 373 K before and after CO oxidation reaction in dry and wet conditions at 318 and 328 K, respectively, are shown in Fig. 13. Note that these reaction conditions are the same as those employed for the intervening activation treatment in Fig. 12 and for the dry condition in Fig. 7. After the treatment, the intensity of the main peak at 0.157 nm was weakened, whereas peaks around 0.270 nm appeared, which are believed to have formed due to reduction of the oxidized gold species into metallic gold. To observe the change in the surface state of gold with CO oxidation, XPS was employed.

**TABLE 3**

**Surface Composition of $Au/Al_2O_3$ Catalysts Calcined at 373 K Obtained by Deconvolution of Au 4*f* Peaks**

| Samples | $Au(OH)_3$ | $Au_2O_3$ | Au metal |
|---|---|---|---|
| Before reaction | 0.23 | 0.43 | 0.34 |
| At maximum activity in the dry condition[a] | 0.20 | 0.31 | 0.49 |
| At steady state in the dry condition[a] | 0.0 | 0.0 | 1.0 |
| At steady state in the wet condition[b] | 0.24 | 0.35 | 0.41 |

[a] CO oxidation at 318 K as in Fig. 7.
[b] CO oxidation at 328 K as in Fig. 12.

Figure 14 compares the Au 4*f* peaks after the reaction in the absence and the presence of water vapor. As described above, $Au(OH)_3$, $Au_2O_3$, and metallic Au were coexisting before the reaction for $Au/Al_2O_3$ catalyst calcined at 373 K as shown in Fig. 14a. The XPS spectrum of $Au/Al_2O_3$ catalyst has three broad peaks as shown in Fig. 14b, where it showed the maximum activity in the dry condition, but only two peaks of metallic Au were observed when $Au/Al_2O_3$ catalyst showed steady-state activity (Fig. 7). In the wet condition, however, three broad peaks were maintained even after reaction. To determine the relative surface fraction of $Au(OH)_3$, $Au_2O_3$, and metallic Au quantitatively, deconvolution of Au 4*f* peaks was conducted, and the results are listed in Table 3. It also showed that the gold phase was transformed from $Au(OH)_3$ and $Au_2O_3$ to metallic Au as CO oxidation went on in the dry condition, yet this phase transformation of Au was suppressed in the wet condition.

## DISCUSSION

$Au/TiO_2$ and $Au/Fe_2O_3$ catalysts showed similar tendencies in catalytic activity with calcination tempertures.

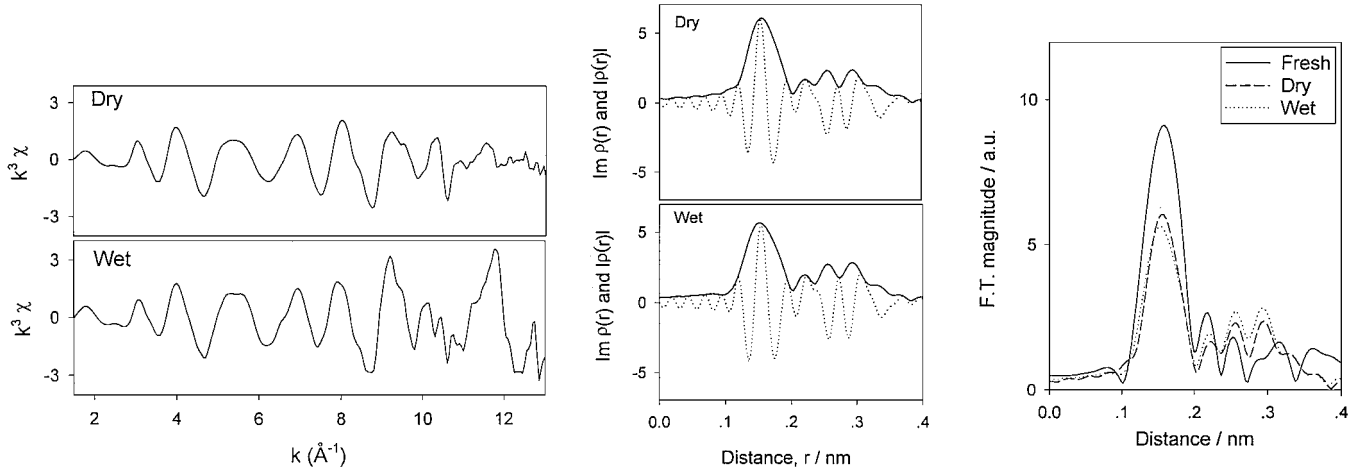


**FIG. 13.** $k^3$-weighted EXAFS functions and their Fourier transformation about the Au $L_{III}$-edge of $Au/Al_2O_3$ calcined at 373 K before CO oxidation, after CO oxidation in the dry condition at 318 K, and after CO oxidation in wet condition at 328 K. The imaginary part of Fourier transform is plotted with dashed lines.

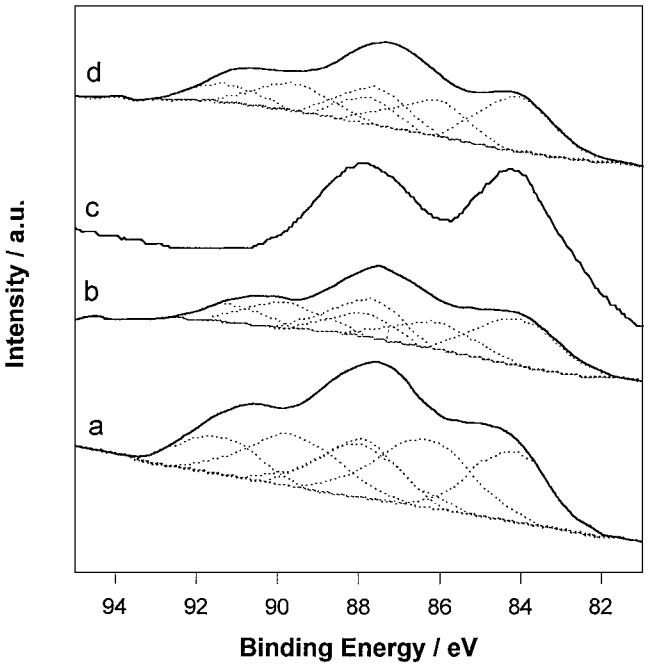


**FIG. 14.** XPS of Au 4*f* obtained for $Au/Al_2O_3$ catalysts calcined at 373 K before and after CO oxidation: (a) before reaction, (b) at maximum activity in the dry condition at 318 K (Fig. 7), (c) at steady state in the dry condition at 318 K, (d) at steady state in the wet condition at 328 K.

These catalysts employ supports most favored by Haruta and co-workers who discovered the activity of these catalysts. As calcination temperatures increased, the CO oxidation activity decreased and the gold phase was changed from $Au(OH)_3$ and $Au_2O_3$ to metallic Au, which was determined by XANES and XPS. For $Au/TiO_2$, Haruta *et al.* (12) reported that the particle size of Au was increased with increasing temperature for calcination in air and that the calcination in reducing gas atmospheres, such as $H_2$ and CO, led to smaller gold particles than in air and that the catalytic activity of $Au/TiO_2$ was sensitive to the structure of the perimeter interface between Au particles and $TiO_2$. Unfortunately they did not report reaction rate data in relation to calcination temperatures. There was no attempt to relate the catalytic activity with the gold phase. Following their view point, the decreasing catalytic activity of $Au/TiO_2$ in the present work with increasing calcination temperatures above 573 K could be understood by the increasing particle size of metallic Au resulting in a decrease in the number of exposed surface metallic gold atoms. However, the unusually high activity of the catalysts calcined below 473 K cannot be explained that way. We found that dorminant phases of gold in these active catalysts were $Au(OH)_3$ and $Au_2O_3$. Therefore, in $Au/TiO_2$, small oxidized gold species such as $Au(OH)_3$ and $Au_2O_3$ are active in CO oxidation.

Most previous studies for $Au/Fe_2O_3$ employed catalysts prepared by the coprecipitation method. Haruta *et al.* (7) showed how gold species in the Au–Fe coprecipitated precursors changed after drying and calcination in air at different temperatures with XAFS. At 473 K and below, gold existed as an oxidized species similar to hydrous gold oxide and $Au_2O_3$. At 573 K the oxidized gold species were mostly decomposed into metallic species. However, at this temperature, the coexistence of oxidized species was also seen in XANES. At 673 K, almost all oxidized gold species was decomposed into metallic species. The change in gold species from oxidic to metallic phase was accompanied by the transformation of amorphous ferric hydroxide into crystalline hematite ($\alpha$-$Fe_2O_3$). They observed that Au–Fe coprecipitate calcined at 573 K showed the maximum activity and concluded that the presence of metallic Au was indispensable for the low-temperature CO oxidation. However, they did not consider the change in the surface gold concentration and surface area with calcination temperatures that should have been accompanied by the change in the phase and surface area of the support itself.

To relate the catalytic activity in CO oxidation directly to the gold phase, $Fe_2O_3$ calcined at 873 K was chosen here as a support and the deposition–precipitation method was selected instead of the coprecipitation method. At least, there will be no significant change in support during calcination after the deposition of gold. As the calcination temperature increased, the catalytic activity decreased and the decreasing activity over $Au/Fe_2O_3$ catalyst calcined at 373 K accompanied the phase transition of gold from the oxidized gold to the metallic gold. Unfortunately, the particle size of Au also increased with increasing calcination temperatures as shown by TEM in Fig. 6 and could also account for the observed change in CO oxidation rates with calcination temperatures. Thus, we can safely state that the effect of the gold phase is at least as important as that of the particle size of the metallic gold. Furthermore, it appears that oxidized gold is more active than metallic gold in CO oxidation. There are several observations that support this proposition. First, catalysts calcined below 573 K showed decreasing catalytic activity at the initial stage and reached a steady-state activity at the reaction temperature of 363 K. This suggests that the active oxidized gold transforms into less active metallic Au during the reaction at this temperature. This was confirmed by the fact that Au 4*f* XPS peaks of $Au/Fe_2O_3$ catalyst at steady state for CO oxidation in dry conditions were the same as those of metallic Au (Fig. 5). Still, the activities of these catalysts were always higher than those catalysts calcined at higher temperatures. Second, the rates of CO oxidation are substantially higher in the wet condition than in the dry condition for all catalysts. It was found by XPS for both $Au/Fe_2O_3$ (Fig. 5) and $Au/Al_2O_3$ (Fig. 14, and Table 3) catalysts that the role of water was to suppress the reduction of oxidized gold to less active metallic gold. Finally, as mentioned earlier, Haruta and co-workers (12) reported that calcination of $Au/TiO_2$ in air gave Au particles larger than those obtained by calcination in the reducing

atmosphere. However, Fig. 2 shows that $Au/TiO_2$ calcined in air is more active than that calcined in $H_2$. Clearly, in this case, the oxidation state of Au is more important for catalytic activity than the particle sizes of Au. There were also some studies that proposed the oxidized gold species as the active sites of Au for CO oxidation. Kang and Wan (24) studied Au/Y-type zeolite prepared by an ion-exchange method and found that the catalyst possessed high catalytic activities for low-temperature CO oxidation without any pretreatment but deactivation was observed. They attributed the deactivation to the transformation of active gold(III) species into gold metal of poor activity. They also assigned the active sites on Au/Fe/Y-zeolite catalysts to gold hydroxide species surrounded by iron oxides (25). Minico *et al.* (26) studied coprecipitated $Au/Fe_2O_3$ catalysts by FT-IR spectroscopy of adsorbed CO and found that in the CO oxidation cationic gold was more active but less stable than the metallic gold. The particle size of Au should also be important when only metallic Au is present. The decreasing catalytic activity with increasing calcination temperatures above 673 K could be understood as due to reduced gold surface areas by enhanced sintering of metallic gold particles.

The $Au/Al_2O_3$ catalyst showed catalytic activity substantially lower than that of the other two catalysts described above. However, the trend of activity change with calcination temperature was similar to that of more active catalysts. An advantage of $Au/Al_2O_3$ is that XAFS analysis is easier on this catalyst due to lower X-ray absorption of $Al_2O_3$ compared to $Fe_2O_3$ and $TiO_2$. Interesting observations were made during CO oxidation over $Au/Al_2O_3$. The catalysts calcined below 473 K showed dramatic increase in activity after a brief treatment at 328 K with the reaction mixture of $CO/O_2/H_2O/N_2$ (Fig. 12). Furthermore, as shown in Fig. 7, $Au/Al_2O_3$ catalysts calcined at 373 and 473 K exhibit increasing activities of CO oxidation with time on stream at 318 K and a maximum followed by decreasing activities. During the activation treatments, XAFS (Fig. 13) and XPS (Table 3) studies revealed that part of the oxidized gold had transformed to the metallic phase. We attribute the apparent activation of initially less active $Au/Al_2O_3$ catalyst to the formation of the so-called well-defined perimeter between gold and alumina that was claimed by Haruta and co-workers (12, 13) to be responsible for the improved activity over $Au/TiO_2$. Thus, physically mixed $Au/TiO_2$ samples (12) and deposition of $TiO_x$ overlayers onto an inactive Au power (15) showed the high catalytic activity after the interface between gold and $TiO_2$ was formed. Kageyama *et al.* (27) observed the presence of Fe atom as the second neighbor at a distance between Au–O and Au–Au distance in RSF. Bonds between gold and support metals in $Au/Mg(OH)_2$, $Au/TiO_2$, and $Au/Al_2O_3$ were also reported in XAFS studies (19, 28). They observed that pH value in the preparation of $Au/TiO_2$ catalyst affected the height of Au–*M* ($M$ = Au, Ti) peaks at 0.18–0.22 nm in RSF, which caused the difference in the catalytic activity (28). We also attempted to observe the Au–Al bond formation by XAFS in Figs. 10 and 13 with little success. The small intensity and complicated multiple peaks in RSF around distance where the peak is expected to appear would have made its observation difficult even if it were indeed present. Instead, both XPS and XAFS indicate that $Au/Al_2O_3$ is partially reduced during the activation processes. This apparent activation of $Au/Al_2O_3$ catalyst was observed only when $Au/Al_2O_3$ catalyst contained oxidized gold. This behavior is not observed for catalysts calcined above 573 K that do not contain oxidized gold in their initial fresh state. During reaction at 328 K, CO is believed to contribute to the reduction of the oxidized gold species. This suggestion is supported by the observation that the activation occurs also after treatment with 1% $CO/N_2$ without $O_2$ at 473 K. Although the mechanism by which CO contributes to the activation is not clear, it may be related to the oxidation–reduction treatments employed by Bollinger *et al.* (14, 15) in order to activate an inactive $Au/TiO_2$ catalyst prepared by an impregnation method.

In CO oxidation over supported gold catalysts, it thus appears that a strong interaction between gold and the support and the formation of the well-defined interface between the two phases are critical for high activity. The preferred supports such as $TiO_2$ and $Fe_2O_3$ form this interface easily during the preparation step, whereas alumina, an inactive support, needs a special treatment for the formation of the interface after preparation.

## CONCLUSIONS

In oxidation of CO at a low temperature, gold catalysts supported on $Fe_2O_3$, $TiO_2$, and $Al_2O_3$ showed the decreasing activity with increasing calcination temperatures with $Al_2O_3$-supported catalyst showing activity substantially lower than that of the other two catalysts. XPS and XAFS studies showed the phase transition of gold from $Au(OH)_3$ through $Au_2O_3$ to metallic Au with increasing calcination temperatures for all catalysts. In addition to the particle size of metallic Au, the oxidation state of gold was proven to be important for CO oxidation. Oxidized gold is more active than metallic gold. Furthermore, facile formation of the interface between gold and support appears to be critical for high CO oxidation activity of supported gold catalysts. $TiO_2$ and $Fe_2O_3$ are favored supports for gold because they form this interface easily while $Al_2O_3$ is ineffective due to its inability to do so.

## ACKNOWLEDGEMENTS

This work has been supported by Pohang Iron and Steel Company and Samsung Petrochemicals Company. XAFS data were collected at Pohang Light Source, Korea, and Photon Factory in the National Laboratory for High Energy Physics (KEK), Japan.

## REFERENCES


1. Schwank, J., *Gold Bull.* **16**, 103 (1983).
2. Haruta, M., *Catal. Today* **36**, 153 (1997).
3. Haruta, M., Kobayashi, T., Sano, H., and Yamada, N., *Chem. Lett.* 405 (1987).
4. Haruta, M., Kageyama, H., Kamijo, N., Kobayashi, T., and Delannay, F., *in* "Successful Design of Catalysts," p. 33. Elsevier, Amsterdam, 1988.
5. Haruta, M., Yamada, N., Kobayashi, T., and Iijima, S., *J. Catal.* **115**, 301 (1989).
6. Cunningham, D. A. H., Kobayashi, T., Kamijo, N., and Haruta, M., *Catal. Lett.* **25**, 257 (1994).
7. Haruta, M., Tsubota, S., Kobauashi, T., Kageyama, H., Genet, M. J., and Delmon, B., *J. Catal.* **144**, 175 (1993).
8. Schryer, D. R., Upchurch, B. T., Norman, J. D. V., Brown, K. G., and Schryer, J., *J. Catal.* **122**, 193 (1990).
9. Choi, K. I., and Vannice, M. A., *J. Catal.* **127**, 489 (1991).
10. Kim, K. D., Nam, I.-S., Chung, J. S., Lee, J. S., Ryu, S. G., and Yang, Y. S., *Appl. Catal. B* **5**, 103 (1994).
11. Park, E. D., and Lee, J. S., *J. Catal.* **180**, 123 (1998).
12. Tsubota, S., Cunningham, D. A. H., Bando, Y., and Haruta, M., *in* "Preparation of Catalysts," Vol. VI, p. 227. Elsevier, Amsterdam,1995.
13. Cunningham, D., Tsubota, S., Kamijo, N., and Haruta, M., *Res. Chem. Interm.* **19**, 1 (1993).
14. Lin, S. D., Bollinger, M., and Vannice, M. A., *Catal. Lett.* **17**, 245 (1993).
15. Bollinger, M., and Vannice, M. A., *Appl. Catal. B* **8**, 417 (1996).
16. Pantelouris, A., Kuper, G., Hormes, J., Feldmann, C., and Jansen, M., *J. Am. Chem. Soc.* **117**, 11,749 (1995).
17. Bassi, I. W., Lytle, F. W., and Parravano, G., *J. Phys. Chem.* **72**, 3563 (1968).
18. Cocco, G., Enzo, S., Fagherazzi, G., Schiffini, L., Bassi, I. W., Vlaic, G., Galvagno, S., and Parravano, G., *J. Phys. Chem.* **83**, 2527 (1979).
19. Kageyama, H., Tsubota, S., Kamijo, N., and Haruta, M., *Jpn. J. Appl. Phys. I* **32**, 445 (1993).
20. Gardner, S. D., Hoflund, G. B., Davidson, M. R., Laitinen, H. A., Schryer, D. R., and Upchurch, B. T., *Langmuir* **7**, 2149 (1991).
21. Epling, W. S., Hoflund, G. B., Weaver, J. F., Tsubota, S., and Haruta, M., *J. Phys. Chem.* **100**, 9929 (1996).
22. Briggs, D., and Seah, M. P., "Practical Surface Analysis," Vol. 1, "Auger and X-ray Photoelectron Spectroscopy," p. 562. Wiley, New York, 1990.
23. Teo, B. K., "EXAFS: Basic Principles and Data Analysis." Springer, Berlin, 1985.
24. Kang, Y.-M., and Wan, B.-Z., *Appl. Catal.* **128**, 53 (1995).
25. Kang, Y.-M., and Wan, B.-Z., *Catal. Today* **26**, 59 (1995).
26. Minico, S., Scire, S., Crisafulli, C., Visco, A. M., and Galvagno, S., *Catal. Lett.* **47**, 273 (1997).
27. Kageyama, H., Kamijo, N., Kobayashi, T., and Haruta, M., *Physica B* **158**, 183 (1989).
28. Kageyama, H., Tsubota, S., Kadono, K., Fukumi, K., Akai, T., Kamijo, N., and Haruta, M., *J. Phys. IV* **7**, 935 (1997).